International Journal of Theoretical and Applied Mathematics
2022; 8(3): 65-77
http://www.sciencepublishinggroup.com/j/ijtam
doi: 10.11648/j.ijtam.20220803.13
ISSN: 2575-5072 (Print); ISSN: 2575-5080 (Online)

Upshot of Slip Velocity and Thermal Radiation on Magnetohydrodynamic Transient Fluid Flow Through Vertical Walls

Bashiru Abdullahi[1, *], Isah Bala Yabo[2], Ibrahim Yakubu Seini[3], Murtala Muhammed Hamza[2]

[1]Department of Mathematics and Statistics, Abdu Gusau Polytechnic, Talata Mafara, Nigeria

[2]Department of Mathematics, Usman Danfodiyo University, Sokoto, Nigeria

[3]Department of Mechanical Engineering, School of Engineering, University for Development Studies, Tamale, Ghana

Email address:

malbashmaf@yahoo.com (Bashiru Abdullahi)

[*]Corresponding author

To cite this article:

Bashiru Abdullahi, Isah Bala Yabo, Ibrahim Yakubu Seini, Murtala Muhammed Hamza. Upshot of Slip Velocity and Thermal Radiation on Magnetohydrodynamic Transient Fluid Flow Through Vertical Walls. *International Journal of Theoretical and Applied Mathematics*. Vol. 8, No. 3, 2022, pp. 65-77. doi: 10.11648/j.ijtam.20220803.13

Received: February 16, 2022; **Accepted**: March 7, 2022; **Published**: September 29, 2022

Abstract: Transient MHD heat transfer within radiative channel due to convective boundary and slip velocity is considered. Non-linear Roseland approximation was used to describe the radiative heat flux in the energy equation where the magnetic field is combined in the momentum equation. The solution of the governing differential equation that described the flow was solved using the Perturbation method in order to obtain the analytical solution which was used to confirm the validity of the numerical solution. The finite difference method was employed to find the numerical solution of the governing equations. The heat transfer device of the present work establishes the influence of Biot number, slip parameter (λ), magnetizing parameter, radiation parameter, temperature difference, Grashof number and time on velocity, temperature, skin friction, and Nusselt number. The results established were discoursed with the aid of line graphs. The steady-state solution was in perfect agreement with the transient form for the weighty value of time t. It is exciting to report that the convective boundary condition and slip velocity has a strong impact on the flow parameters.

Keywords: MHD, Slip Velocity, Thermal Radiation, Heat Transfer, Convective Boundary Condition

1. Introduction

Numerous scholars surveyed no-slip boundary states under certain circumstances. No-slip condition is not appropriate in some situations and is replaced by a partial slip condition. In their study, Venkateswarlu and Venkata [1] stated that fluid slip boundary situation arises in many submissions such as in micro-channels or Nano-channels and it is applied where a thin film of light oil is attached to the moving plates or when the surface is coated with special coatings such as thick monolayer of hydrophobic octadecyl trichlorosilane. Slip boundary conditions are also applied in the enhancing of synthetic heart regulators and interior crevices, fluid motion within the human body, etc. Many researchers, considering the application of slip velocity and convective boundary condition in science and technology conducted research on the subject matter: [2-16].

Thermal radiation impact on free convection heat transfer flow problems on MHD continues to have an exciting pact of apprehension. Dulal and Babulal [17] describe the radiation effect as quite significant at a high working temperature such as appropriate equipment in the designs of aircraft, missiles, satellites, and space vehicles. Several researchers have studied the influence of thermal radiation on MHD free- convection in combination with other flow parameters. Misra and Sinh [18] discussed theoretical analysis on Magnetohydrodynamics flow of blood in a vessel, in which thermal radiation, velocity slip, and thermal slip conditions are taken into consideration. It was found that thermal radiation (R) stands prospective to convey a significant change in the temperature field of the boundary layer. Mathematical analysis of MHD flow and heat transfer from a warm, electrically conducting fluid to a melting surface

moving parallel to a constant free stream in the presence of thermal radiation was deliberated by Kalidas [19]. It was detected that the fluid temperature and the thermal boundary layer thickness decline for growing thermal radiation, melting parameter and magnetic field whereas reverse effect occurs for moving parameter. Kho et al [20] debated on boundary layer flow of Williamson Nanofluids past over a stretching sheet in the presence of thermal radiation effect. It was established that radiation parameters influenced both temperature profile and the rate of heat transfer. Isah *et al*. [21] studied Couette flow under the influence of the transverse magnetic field and thermal radiation for a nonlinear coupled system of two infinite vertical plates held at different temperatures.

Inspired by the above studies, this research intended to improve the work of Isah *et al.* [21] to incorporate velocity slip and convective temperature at the boundary in the presence of thermal radiation and to investigate their influences on free convective heat transfer flow of MHD using non-linearized Roseland approximation.

2. Mathematical Analysis

Formation of steady/transient laminar, non-compressible, and conducting fluid (MHD) flow between two vertical parallel plates in the existence of a magnetic field of strength B_0 is considered. The x'-axis is taken in the track of main flow along with the plate and the y'-axis is normal to the plate. Prior to the startup (dimensional time t' less than or equal to zero) of the experiment the fluid and plate are assumed to be at rest at constant temperature T_0. At startup (dimensional time t' greater zero) the temperature of the plate situated at the left plate (y' = 0), received a convection energy $-k^*\frac{\partial T'}{\partial y'}\Big|_{y'=0} = h_1[T_1 - T'(0,t)]$ with slip velocity $\left(u' = \gamma^*\frac{\partial u'}{\partial y}\right)$ while reference temperature at the right plate (y' = H) is maintained as T_0 see figure 1. Under Boussinesq approximation and conceited the flow to be laminar and fully developed, the boundary-layer velocity and temperature equations (in the dimensional form) are respectively given below:

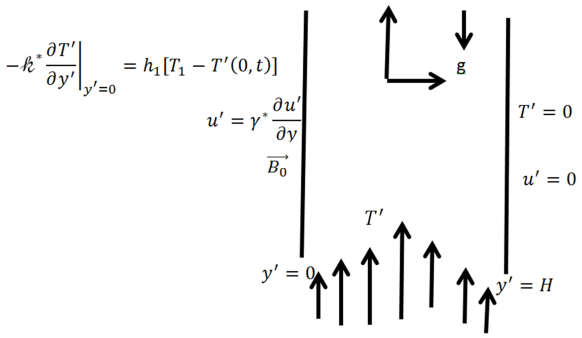

Figure 1. *Geometry of the problem.*

$$\frac{\partial u'}{\partial t'} = \nu\frac{\partial^2 u'}{\partial y'^2} + g\beta(T_1 - T_0) - \sigma\frac{\beta_0 u'}{\rho} \quad (1)$$

$$\frac{\partial T'}{\partial t'} = \alpha\left[\frac{\partial^2 T'}{\partial y'^2} - \frac{1}{K}\frac{\partial q_y}{\partial y'}\right] \quad (2)$$

Where:
α = thermal diffusivity,
K = thermal conductivity,
β = coefficient of the thermal expansion
σ = fluid electrical conductivity,
g = gravitational acceleration
B_0 = strength of applied magnetic field.
Initial and channel boundary situations are given as:

$$\left.\begin{array}{c} t' \le 0: for\ 0 \le y' \le H, u' = 0;\ T' = T_0 \\ t' > 0: u' = \gamma^*\frac{\partial u'}{\partial y}, -k^*\frac{\partial T'}{\partial y'}\Big|_{y'=0} = h_1[T_1 - T'(0,t)], at\ y' = 0 \\ u' = 0, T' = T_0, at\ y' = H \end{array}\right\} \quad (3)$$

The following dimensionless quantities are introduced:

$$t = \frac{t'\nu}{H^2}, y = \frac{y'}{H}, P_r = \frac{\nu}{\alpha}, \theta = \frac{T' - T_0}{T_1 - T_0}, B_{i1} = \frac{h_1 H}{k^*}, G_r = \frac{[g\beta H^2(T_1 - T_0)]}{\nu U}, M^2 = \frac{\sigma\beta_0^2 H^2}{\rho\nu},$$

$$u = \frac{u'}{U}, \gamma = \frac{\gamma^*}{H} \quad (4)$$

Simplifying radiation heat flux in the problem, Roseland approximation is used:

$$q_y = \frac{-4\sigma\partial T'^4}{3k^*\partial y'} \quad (5)$$

Expanding T'^4 into the Taylor series expansion in order to linearized equation (5) we have:

$$T'^4 = (\theta(T_1 - T_0) + T_0)^4 \quad (6)$$

Using equations (5) and (6) into dimensional equations (1) and (2) due to condition (3) the dimensionless form of the velocity and temperature equations are respectively found to be:

$$\frac{\partial u}{\partial t} = \frac{\partial^2 u}{\partial y^2} + Gr\theta - M^2 u \quad (7)$$

$$P_r\frac{\partial\theta}{\partial t} = \left[1 + \frac{4R}{3}(C_T + \theta)^3\right]\frac{\partial^2\theta}{\partial y^2} + 4R[C_T + \theta]^2\left(\frac{\partial\theta}{\partial y}\right)^2 \quad (8)$$

With fresh initial and boundary conditions:

$$\left.\begin{array}{c} t \le 0, 0 \le y \le 1: u = 0;\ \theta = 0 \\ t > 0, y = 0: u = \gamma\frac{\partial u}{\partial y}, -\frac{\partial\theta}{\partial y}\Big|_{y=0} = B_{i1}[1 - \theta], \\ y = 1: u = 0, \theta = 0 \end{array}\right\} \quad (9)$$

3. Analytical Solution

Analytical solutions are very essential in validating a time dependent (numerical) solution of heat transfer flow of Magnetohydrodynamic. Radiative heat flux that was defined by the Rosseland approximation in the temperature equation cracks the present physical problem highly nonlinear and show no closed form solution. Employing perturbation series method one can obtained the steady state version of (7) and (8) by relaxing time gradients $(\frac{\partial u}{\partial t}, \frac{\partial \theta}{\partial t})$, to zero such that:

$$\frac{d^2u}{dy^2} + Gr\theta - M^2u = 0 \tag{10}$$

$$\left[1 + \frac{4R}{3} + (C_T + \theta)^3\right]\frac{d^2\theta}{dy^2} + 4R[C_T + \theta]^2\left(\frac{d\theta}{dy}\right)^2 = 0 \tag{11}$$

With new boundary conditions:

$$\left.\begin{array}{c} at\ y = 0: u = \gamma\frac{du}{dy}, -\frac{d\theta}{dy} = B_{i1}(1+\theta) \\ at\ y = 1: u = 0, \theta = 0 \end{array}\right\} \tag{12}$$

Using power series expansion and disregarding R^j for $j > 1$ and employ a regular perturbation method, the velocity (u), and temperature (θ) are estimated as;

$$u(y) = \sum_{j=0}^{\infty} R^j u_j(y) \tag{13}$$

$$\theta(y) = \sum_{j=0}^{\infty} R^j \theta_j(y) \tag{14}$$

Now the required steady state solution from (10) to (12) for the velocity and temperature equations can be achieved using equation (13) and (14) as:

$$u(y) = a_3e^{My} + a_4e^{-My} + \frac{Gra_1}{M^2}y + \frac{Gra_2}{M^2} + R(e_1e^{My} + e_2e^{-My} + k_1y^4 + k_2y^3 + k_3y^2 + k_4y + k_5) \tag{15}$$

$$\theta(y) = a_1y + a_2 + R(c_1y^4 + c_2y^3 + c_3y^2 + c_4y + c_5) \tag{16}$$

From (15) the steady state skin frictions at the boundaries are:

$$\tau_0 = \left.\frac{du}{dy}\right|_{y=0} = Ma_3 + a_4 + \frac{a_1}{M^2} + Re_1M - Re_2M + Rk_4 \tag{17}$$

$$\tau_1 = \left.\frac{du}{dy}\right|_{y=1} = a_3e^M - Ma_4e^{-M} + \frac{a_1}{M^2} + R(Me_1e^M - Me_2e^{-M} + 4k_1y^3 + 3k_2y^2 + 2k_3y + k_4 \tag{18}$$

Equally the steady state Nusselt numbers at the boundaries are derived from (16) as:

$$N_{u_0} = \left.\frac{d\theta}{dy}\right|_{y=0} = a_1 + Rc_4 \tag{19}$$

$$N_{u_1} = \left.\frac{d\theta}{dy}\right|_{y=1} = a_1 + 4Rc_1 + 3Rc_2 + 2Rc_3 + c_4 \tag{20}$$

4. Numerical Solution

The present physical model (equation 7 and 8) is extremely nonlinear and coupled. To solve the said equation together with the initial and boundary condition (9) implicit finite difference method was used. The grid spacing (i, j) in y and t are noted as (Isah et *al.* [21]):

$$\frac{u_i^{j+1} - u_i^j}{\Delta t} = \left[\frac{u_{i-1}^{j+1} - 2u_i^{j+1} + u_{i+1}^{j+1}}{(\Delta y)^2}\right] + G_r\theta_i^j - M^2u_i^j \tag{21}$$

$$P_r\frac{\theta_i^{j+1} - \theta_i^j}{\Delta t} = \left[1 + \frac{4R}{3}\left(C_T + \theta_i^j\right)^3\right]\left[\frac{u_{i-1}^{j+1} - 2u_i^{j+1} + u_{i+1}^{j+1}}{(\Delta y)^2}\right] + 4R\left[C_T + \theta_i^j\right]^2\left(\frac{\theta_{i-1}^j - \theta_{i+1}^j}{2\Delta y}\right)^2 \tag{22}$$

With boundary conditions:

$$\left.\begin{array}{c} u_{i-1}^{j+1} = \gamma\left[\frac{-3u_{i-1}^{j+1} + 4u_i^{j+1} - u_{i+1}^{j+1}}{2\Delta y}\right] \\ -\left[\frac{-3\theta_{i-1}^{j+1} + 4\theta_i^{j+1} - \theta_{i+1}^{j+1}}{2\Delta y}\right] = B_{i1}\left[1 - \theta_i^j\right] for\ all\ i = 0 \\ -\left[\frac{-3\theta_{i-1}^{j+1} + 4\theta_i^{j+1} - \theta_{i+1}^{j+1}}{2\Delta y}\right] = B_{i1}\left[1 - \theta_i^j\right] \\ u_M^j = 0, \theta_M^j = 0, \text{for all i} = \text{M} \end{array}\right\} \tag{23}$$

Summarizing and modifying equations (21) and (22) we have;

$$B_l u_{i-1}^{j+1} + B_c u_i^{j+1} + B_r u_{i+1}^{j+1} = r_1 u_{i-1}^{j} - r_1 u_{i+1}^{j} + (1 - \Delta t M^2) u_i^j + \Delta t Gr \theta_i^j \quad (24)$$

$$A_l \theta_{i-1}^{j+1} + A_c \theta_i^{j+1} + A_r \theta_{i+1}^{j+1} = Pr \theta_i^j + \Pr r_1 \theta_{i+1}^j - \Pr r_1 \theta_{i-1}^j + z_2 r_3 \left(\theta_{i-1}^j - \theta_{i+1}^j\right)^2 \quad (25)$$

Since the values of u_0^{j+1}, θ_0^j and θ_0^{j+1} at y = 0 are not defined from the boundary condition (23), One can modify equation (24) and (25) using (23) for $i = 1$ to have;

$$\left(\frac{4B_l}{3} - \frac{2\Delta y B_l}{3\gamma} + Bc\right) u_1^{j+1} + \left(Br - \frac{Bl}{3}\right) u_2^{j+1} = (1 - \Delta t M^2) u_1^j + \Delta t \theta_1^j \quad (26)$$

$$\left[\frac{(4-2\Delta y B_{i1})}{3} + A_l\right] \theta_1^{j+1} + \left[A_r - \frac{Al}{3}\right] \theta_2^{j+1} + \frac{2}{3} A_l \Delta y B_{i1} = P_r \theta_1^j + r_2 \left[\frac{(4-2\Delta y B_{i1})}{3} \theta_1^j - \frac{4}{3}\theta_2^j + \frac{2}{3}\Delta y B_{i1} - \theta_2^j\right]^2 \quad (27)$$

5. Result Validation

In order to guarantee the precision of the applied numerical scheme the calculated values of time dependent (numerical) solution of velocity and temperature profiles are compared with the available results of analytical solution obtained using regular perturbation method. It can be seen from figures 2a and b that the two solutions remarkably agreed for sufficiently large value of time t.

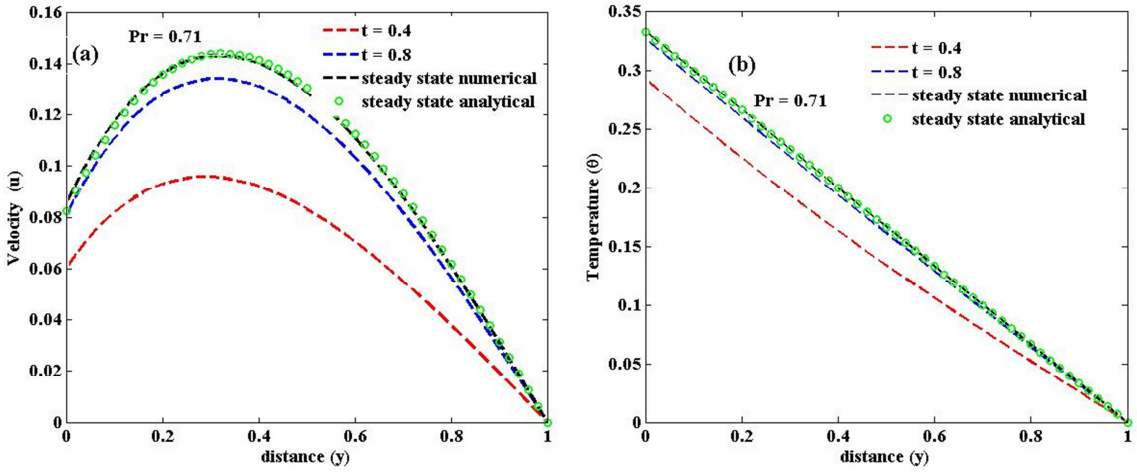

Figure 2. *Consequence of time on steady state velocity and temperature.*

6. Results and Discussions

The present work, studies the steady/unsteady state free convective heat transfer flow through vertical plates taking thermal radiation into consideration, under the impact of a uniform magnetic field subject to slip velocity and convective temperature at the boundary. The system of leading equations (7) and (8) with the boundary conditions (9) is solved using perturbation series method to obtain the analytical solution, whereas implicit finite difference method was used to obtain the numerical solution. The outcome of the flow governing parameters on velocity u(y, t), temperature $\theta(y,t)$, skin friction $(\tau_{0,1})$ and Nusselt number $(Nu_{0,1})$, have been discussed using line graphs as shown from figures 2 to 23. These results display the variations in the u(y, t), $\theta(y,t)$, $(\tau_{0,1})$ and $(Nu_{0,1})$ are subjective by the material flow parameters that is, the magnetic parameter (M), radiation parameter (R), temperature difference parameter (C_T), Prandtl number (Pr), Biot numbers (B_{i1}), slip parameter (λ) and Grashof number (Gr). Prandtl number 0.71 and 7.0, were used to signify physical feature of air and water respectively, while all other parameters are choosing arbitrary.

Velocity profile:

Figures 2 to 7 shows the upshot of dimensionless flow parameters on the velocity outline. Figures 2a and b validates the influence of time on steady state condition of velocity and temperature profiles respectively. The time dependent solution merged with steady state solution for sufficient value of time t which verified the strength and efficiency of the numerical solution. Figures 3a and b shows the sway of Gr on $u(y,t)$. The value of Gr was taken as positive, negative and zeros in order to show the state of the plates. $Gr > 0$ indicate outward cooling of the touching wall while $Gr < 0$ specify the exterior heating of the moving wall. It is observed from the figure that velocity upsurge with growing Gr. As it was reported by Isah et *al.* [21] that "$Gr = 0$ designate a corporeal circumstances when the flow is only due to the drive of one of the boundary". Figure 4a and b describes the upshot of B_{i1} on velocity contour. It is observed from the figure, as B_{i1} decreases and approaches

zero the velocity also declines and diminishes. This is because the thermal resistance of the fluid exceed the thermal resistance presented by the flow wall. Figure 5a and b illustrates the impact of λ on the velocity profile. Velocity enhances with increasing λ. Consequence of M on the velocity distribution is described by figure 6a and b. It shows that velocity decline with growing M. This is because the magnetizing field employs impeding force on the flow. Figure 7a and b demonstrate the impact of R on velocity profile. Velocity boosts with upsurge in R.

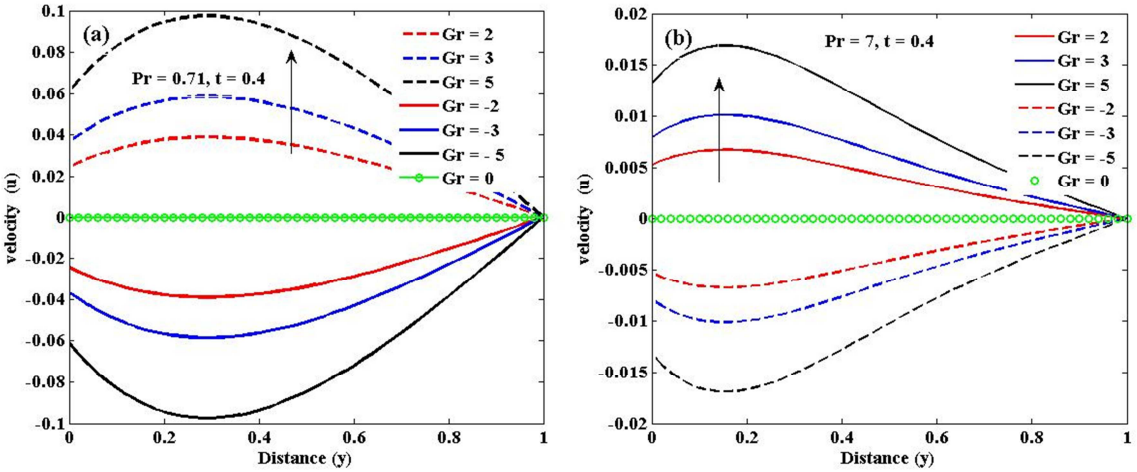

Figure 3. *Consequence of Gr on u(y,t).*

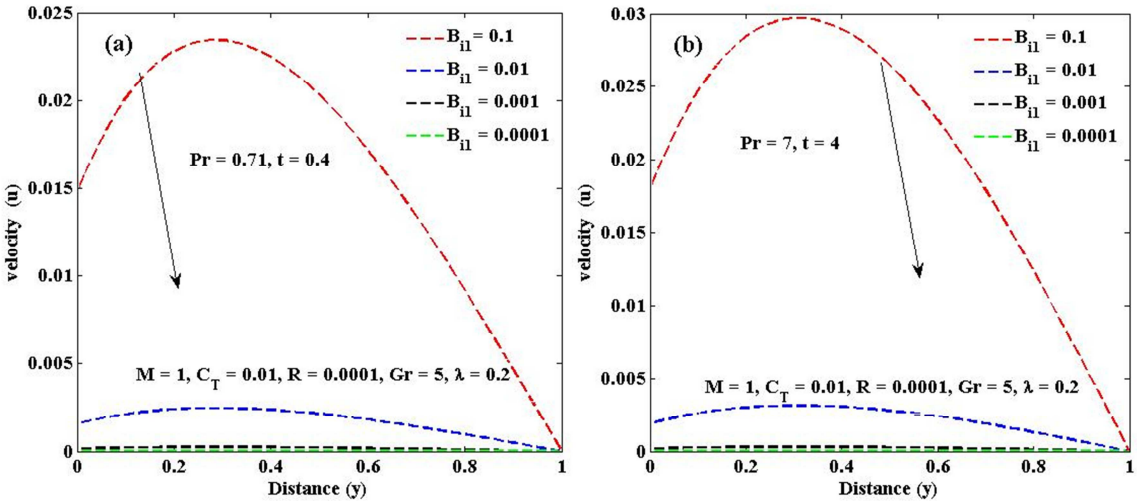

Figure 4. *Consequence of B_{i1} on u(y, t).*

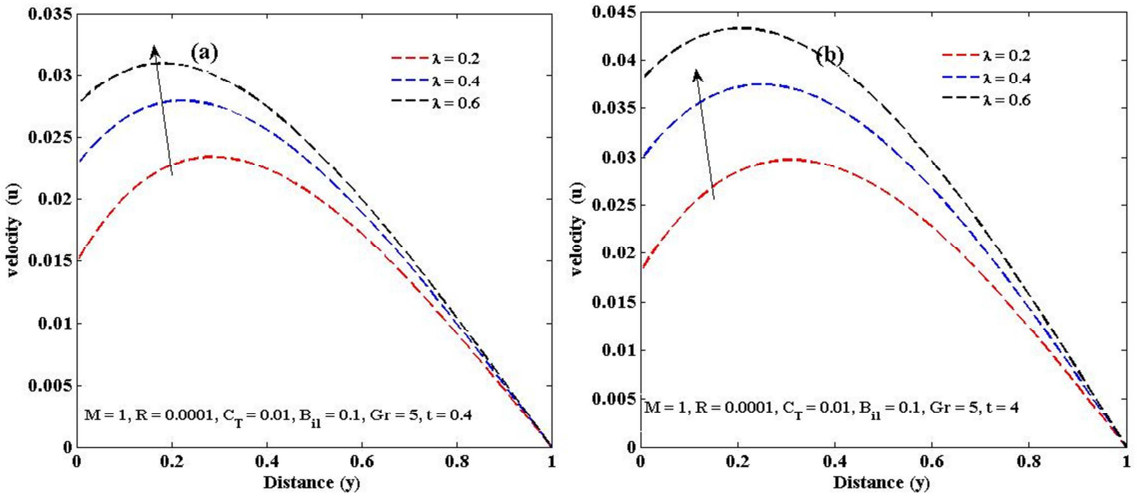

Figure 5. *Consequence of λ on u(y, t).*

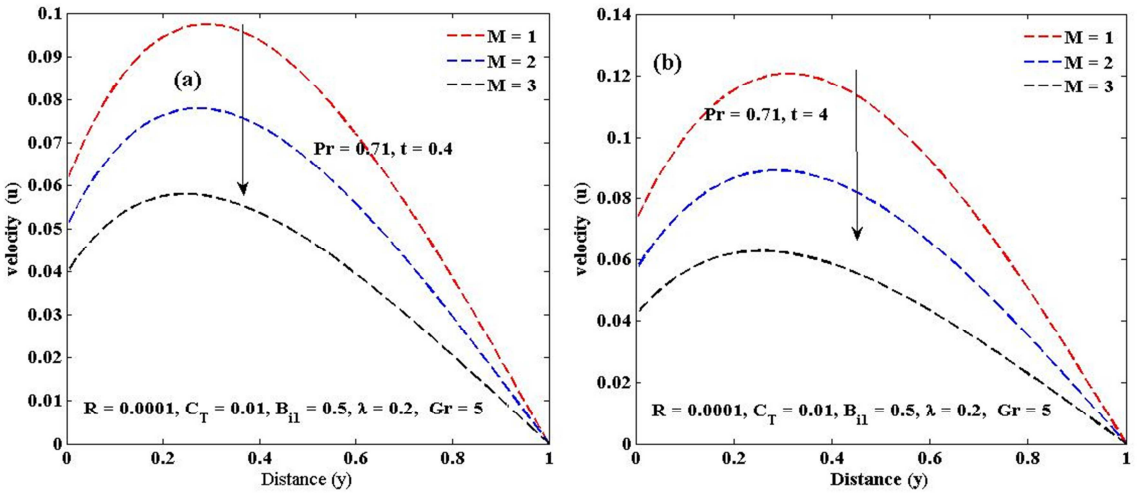

Figure 6. *Consequence of M on u(y, t).*

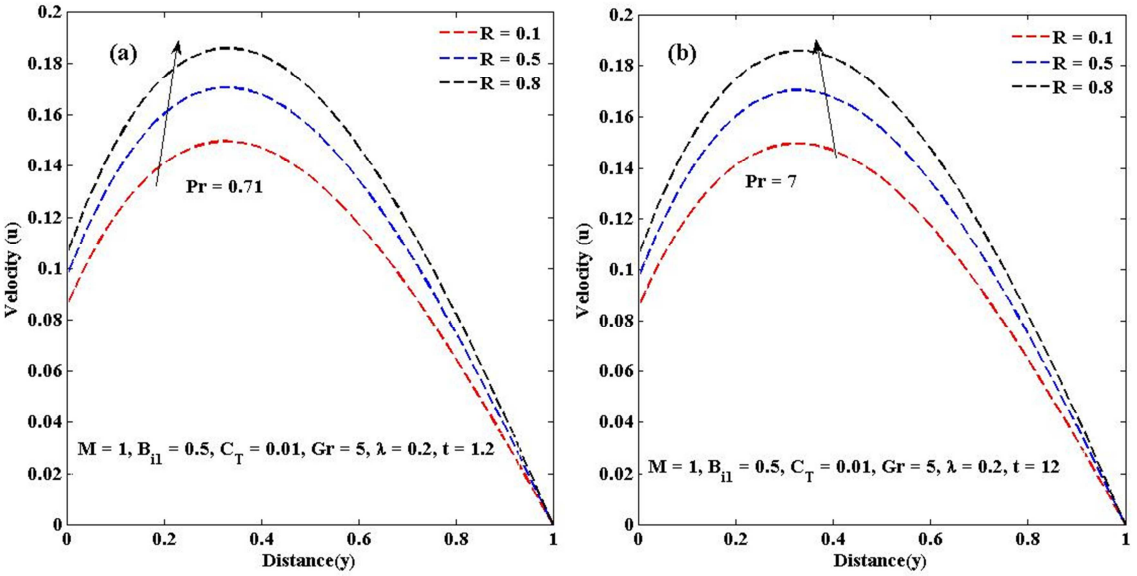

Figure 7. *Consequence of R on u(y, t).*

Temperature profile

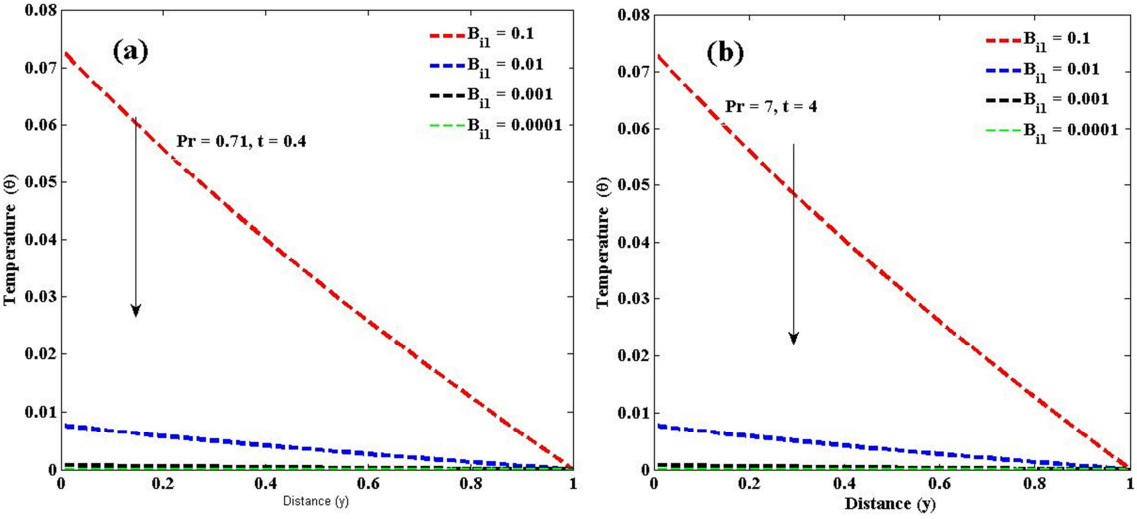

Figure 8. *Consequence of B_{i1} on $\theta(y,t)$.*

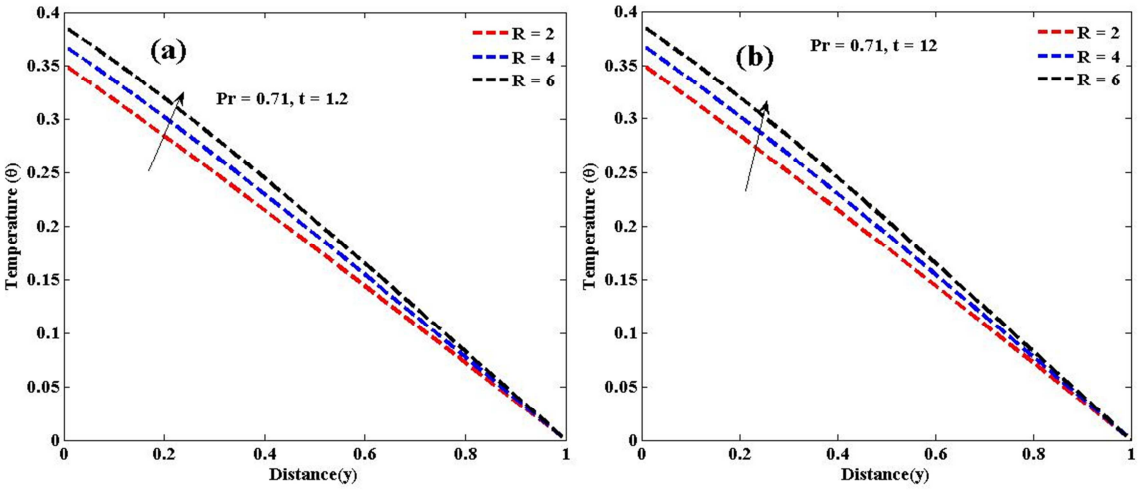

Figure 9. *Consequence of R on* $\theta(y,t)$.

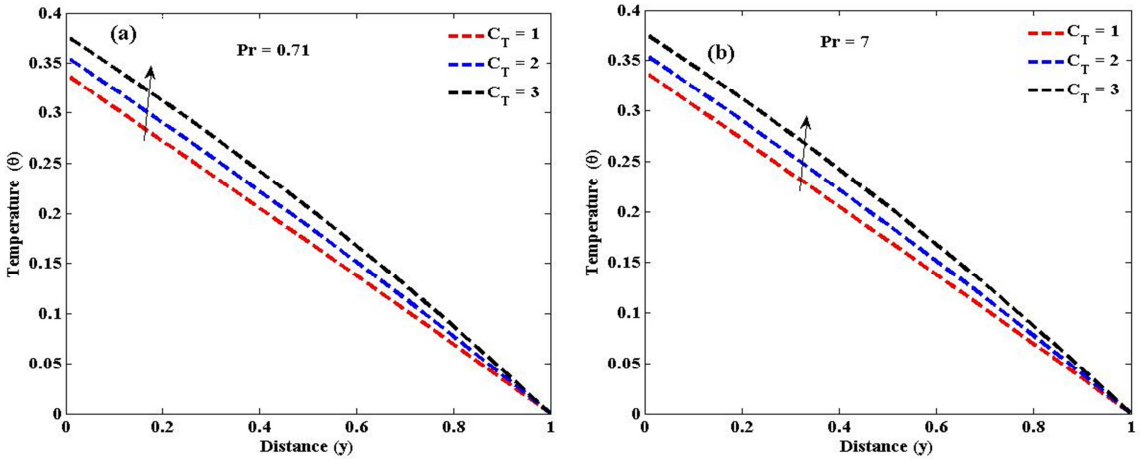

Figure 10. *Consequence of* C_T *on* $\theta(y,t)$.

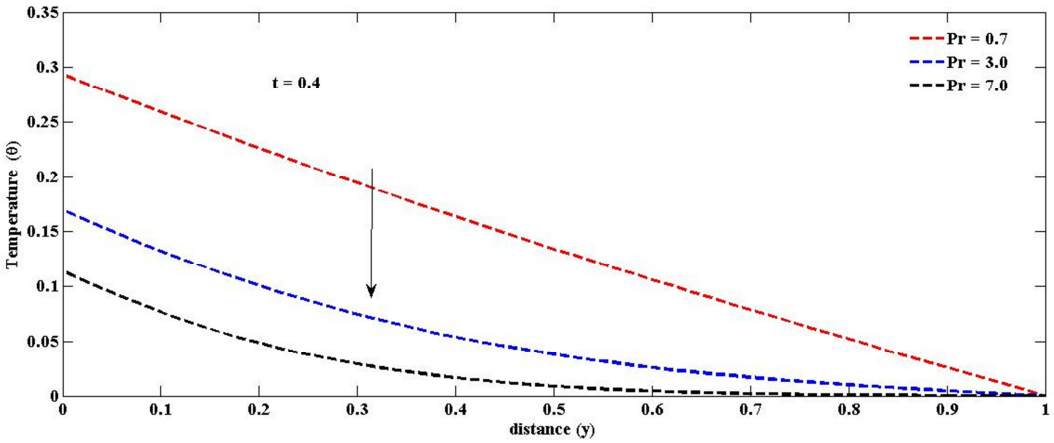

Figure 11. *Consequence of Pr on* $\theta(y,t)$.

Figures 8 to 11 illustrate the effect of dimensionless controlling parameters on $\theta(y,t)$. Sway of B_{i1} on $\theta(y,t)$ has been discussed in figure 8a and b. It is observed that temperature decays as B_{i1} is dropping. The reason behind this is that, the internal convective resistance of the convective wall is comparatively lower than the external resistance and therefore the temperature decays. Figure 9a and b show the upshot of R on temperature outline and it is observed that temperature rises with growing R. Figure 10a and b defines the impact of C_T on temperature outline for air and water respectively. It indicates that, temperature enhances with increasing C_T. Sway of Pr on temperature outline has been discussed in figure 11. It is witnessed that temperature decrease with growing Pr. Obviously it is

exciting that the consequence of Pr is to relaxed the temperature of the fluid, as it upsurges and also to decline the thickness of thermal boundary layer.

Skin friction

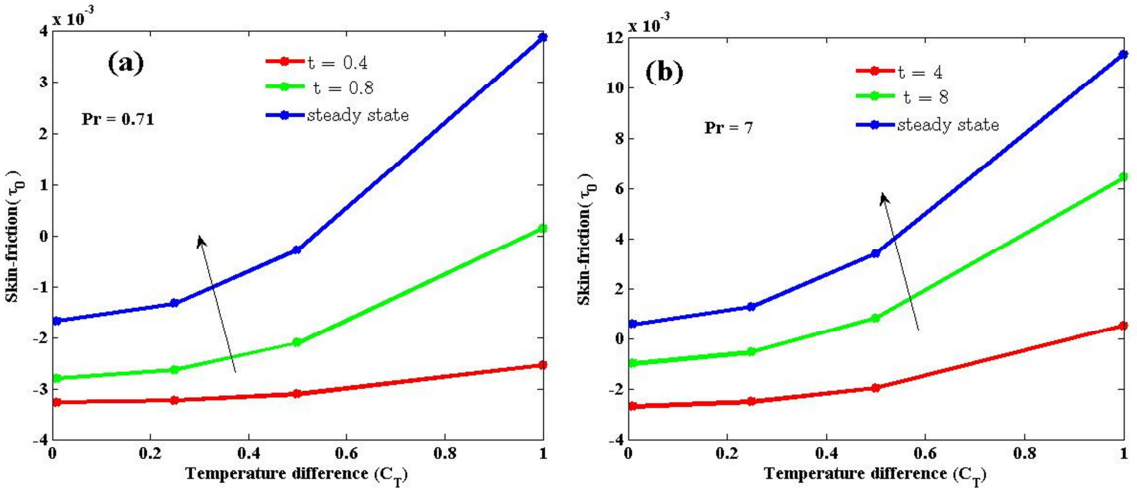

Figure 12. *Sway of time t with rising C_T on skin friction at convective wall.*

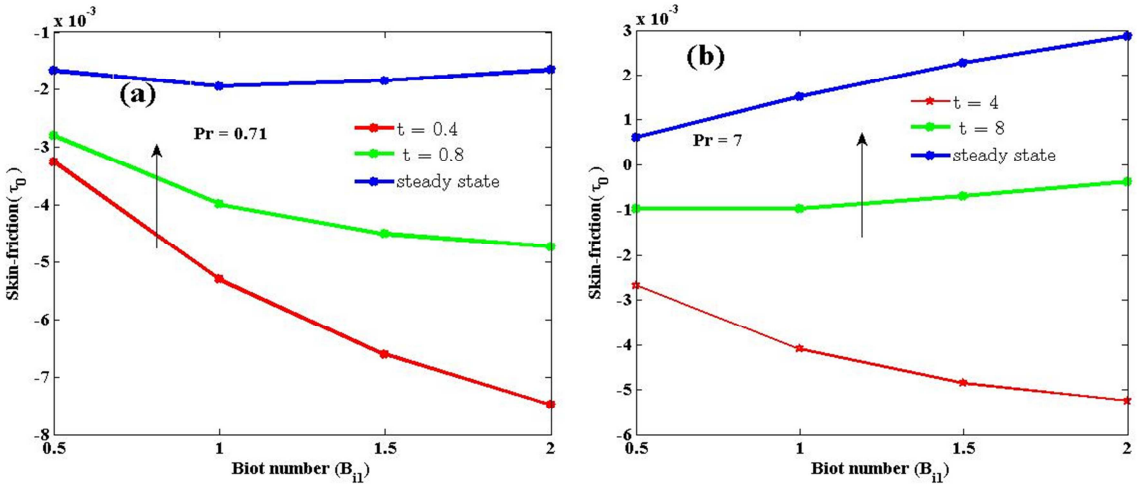

Figure 13. *Sway of time t with rising B_{i1} on skin friction at convective wall.*

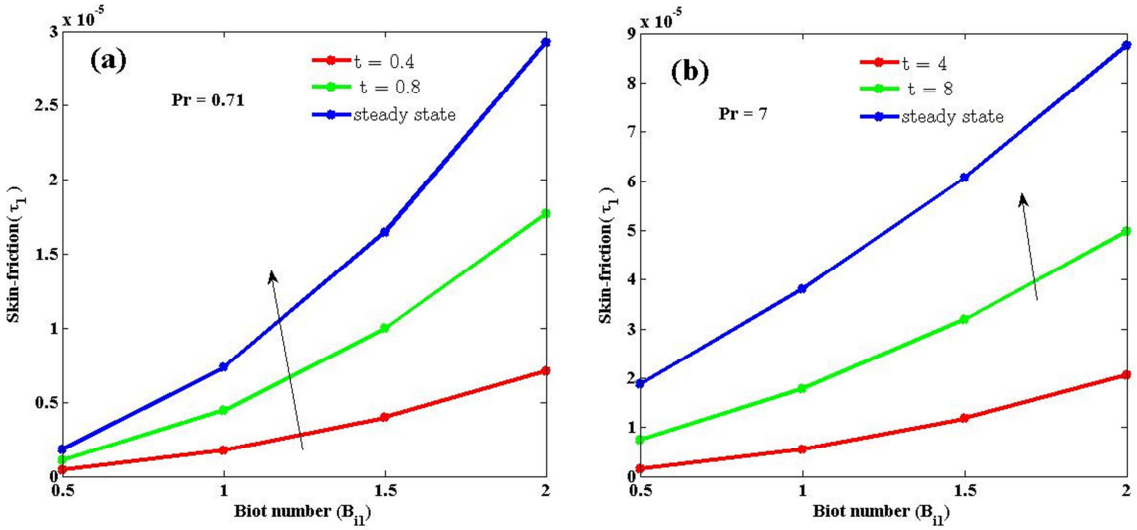

Figure 14. *Sway of time t with rising B_{i1} on skin friction at non-convective wall.*

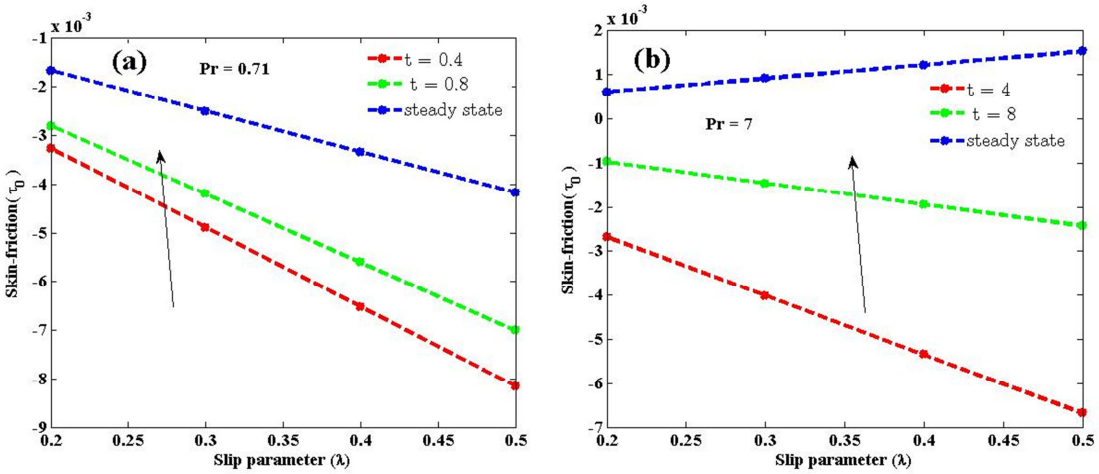

Figure 15. *Sway of time t with rising λ on skin friction at convective wall.*

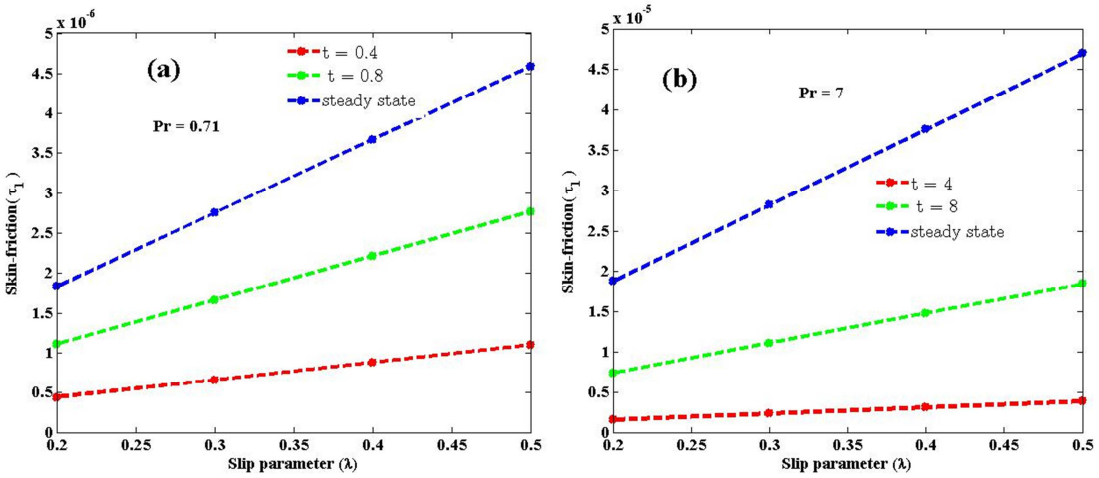

Figure 16. *Sway of time t with rising λ on skin friction at non-convective wall.*

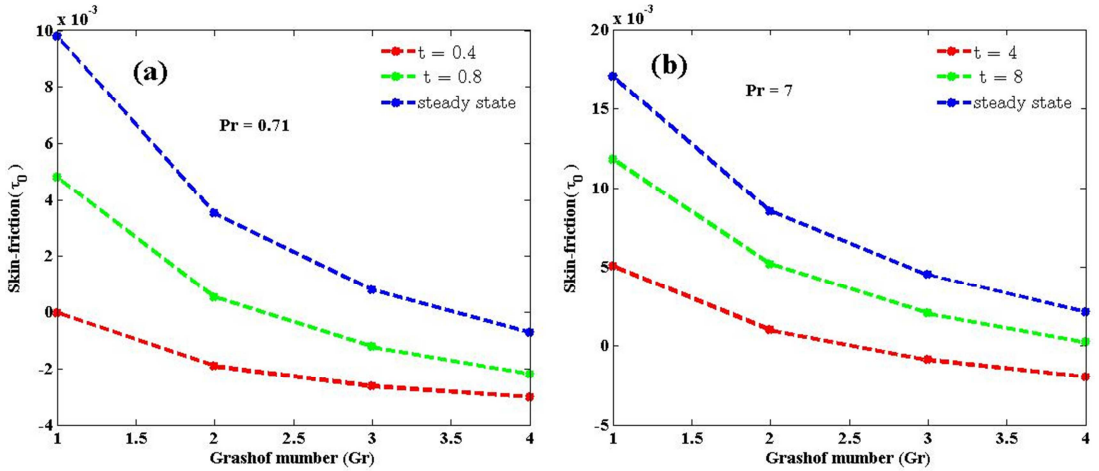

Figure 17. *Sway of time t with rising Gr on skin friction at convective wall.*

Effects of dimensionless controlling parameters on skin frictions are discussed in figures 12 to 19. Figure 12a and b explains the sway of time and C_T on τ_0. As time t and C_T upsurge, τ_0 also rises and achieves steady state for large value of t. The Effect of B_{i1} and time t on τ_0 has been deliberated in 13a and b. τ_0 declines with increasing B_{i1} but boosts with growing time and attains steady state. Moreover influence of B_{i1} and time t on $\tau_1$has be depicted in figure 14a (Pr = 0.71) and b(Pr = 7.0). τ_1 rises with advancing B_{i1} and time t and also reach a steady state for large t. Figures 15 and 16 display the sway of λ and time t on τ_0 and τ_1 respectively. It is perceived that increase in λ leads to decline in τ_0 but upsurge in τ_1. However, in both cases, τ_0 and τ_1 grow with growing time t. Figure 17a and b demonstrates the

consequence of Gr and t on τ_0. It is obseved that τ_0 decrease with increasing Gr but upsuge with rising time and reached steady state for large values of t. Figure 18a and b illustrate the upshot of M and B_{i1} on τ_0. It is observed that for both air (18a) and water (18b) τ_0 increase with increasing M but decrease with increasing B_{i1}. Figure 19a and b demostrate the effect of R on τ_1. It is observed that, skin friction enhances with increasing R.

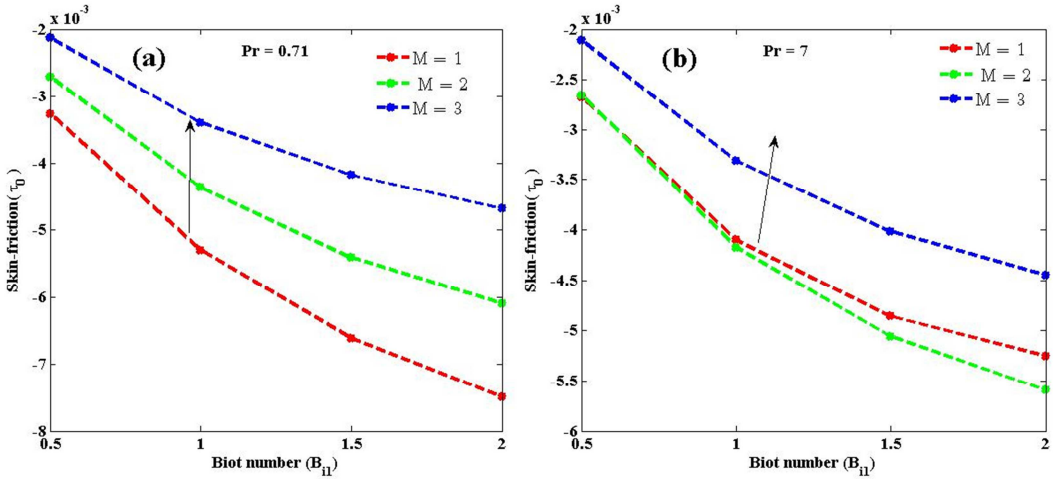

Figure 18. *Sway of M with risingB_{i1} on skin friction at convective wall.*

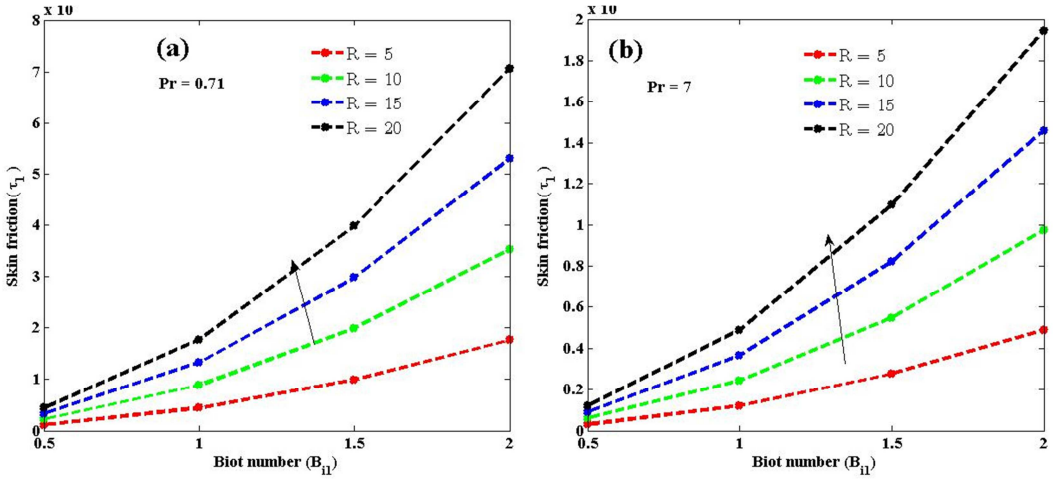

Figure 19. *Sway of R with rising B_{i1} on skin friction at non-convective wall.*

Nusselt number

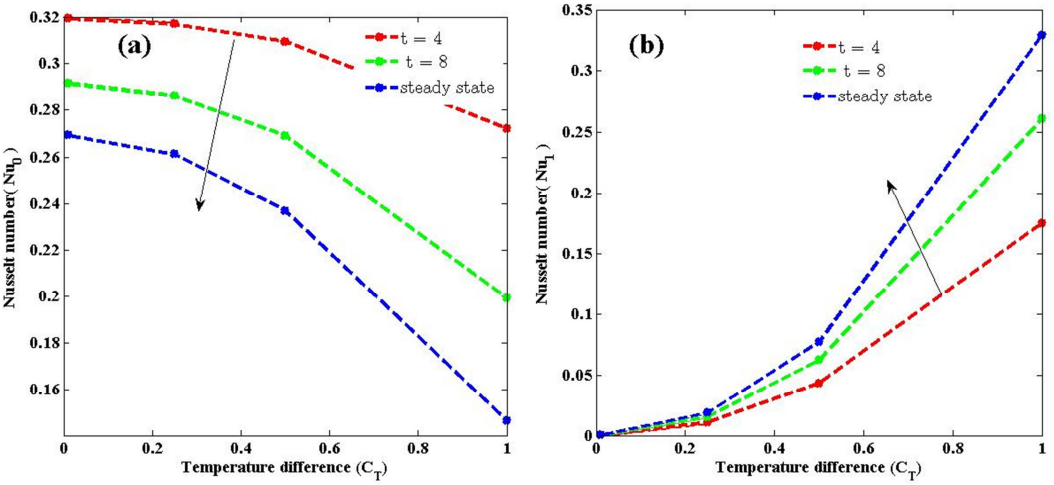

Figure 20. *Nusselt number against $C_T$with increasing time t (Pr = 7.0).*

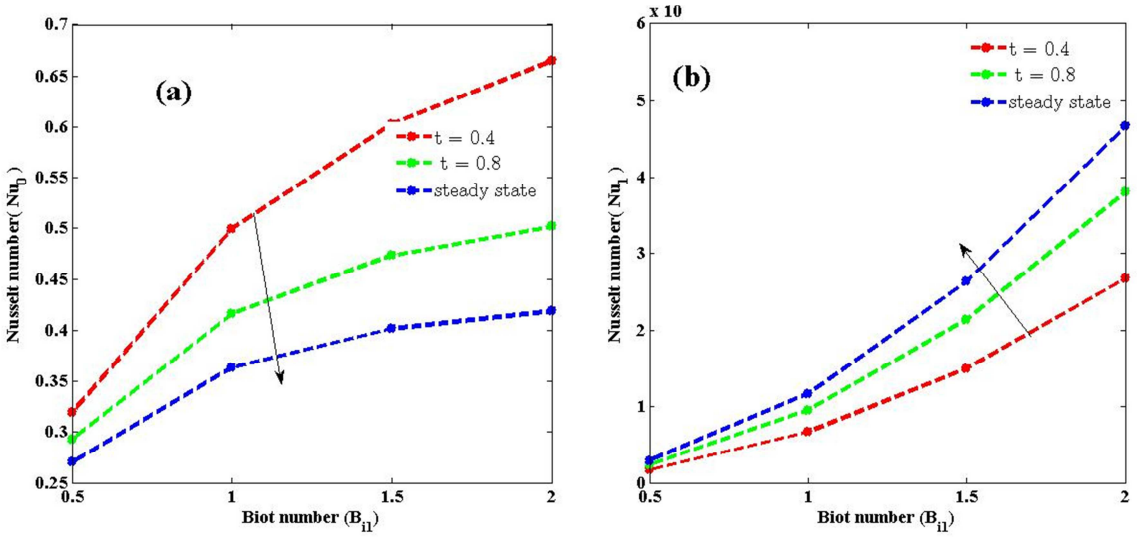

Figure 21. *Nusselt number against B_{i1} with increasing time t (Pr = 0.71).*

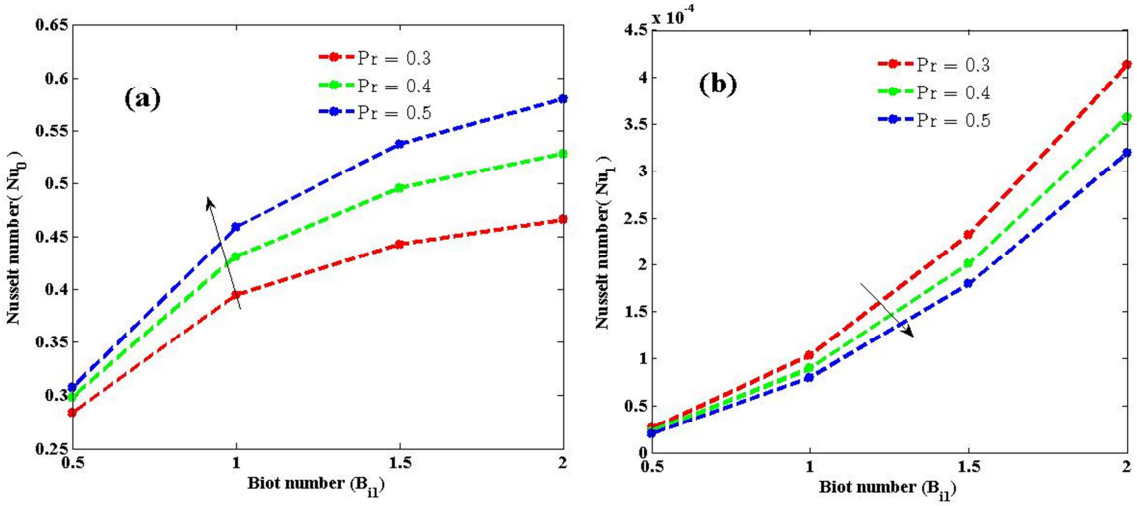

Figure 22. *Nusselt number against B_{i1} with increasing Pr.*

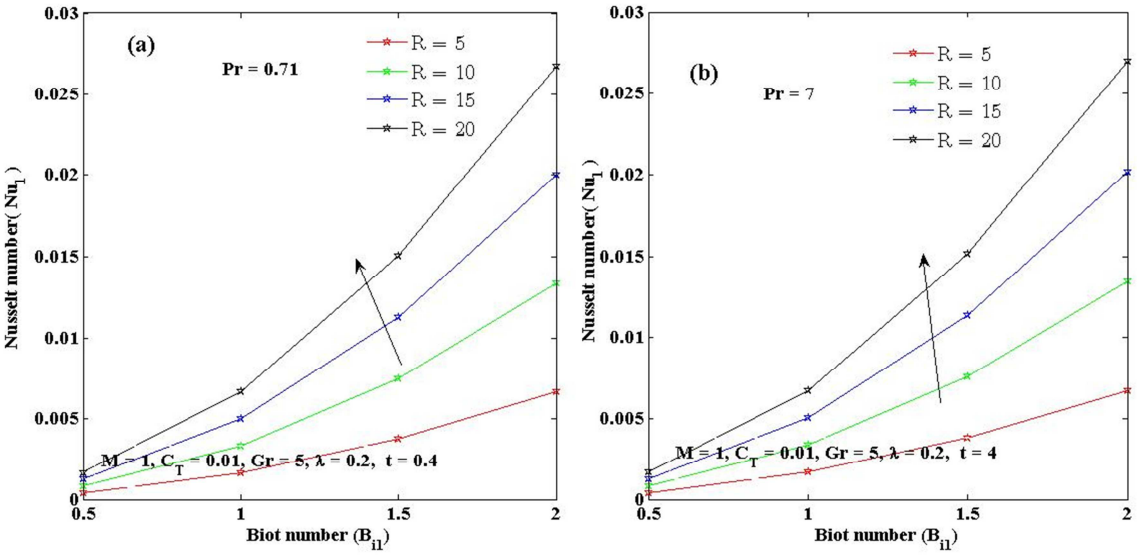

Figure 23. *Nusselt number against B_{i1} with increasing R.*

Figures 20 to 23 indicate the influence of dimensionless controlling parameters on Nusselt numbers (Nu_0 and Nu_1).

Influence of time and C_T on Nu_0 and Nu_1 is discussed in figure 20a and b respectively. It is observed that, at convective plate (y = 0), Nu_0 decreases with increasing time t and C_T and reaches steady state for growing values of time t while other controlling parameters assume fixed values; whereas Nu_1 enhances with increasing time t and C_T and also attains steady state for sufficient values of time t. Figure 21a and b displays the upshot of B_{i1} and time t on Nu_0. It is experimentally perceived that rise in B_{i1} lead to upturn in Nu_0. Figure 22a and b illustrate the influence of Pr andB_{i1} on Nu_0. It is indicated that, at convective plate ($y = 0$), increase in Pr and B_{i1} leads to upturn in Nu_0, but Nu_1 decline when Pr is growing but increase with rising B_{i1}. Figure 23a and b demonstrate the sway of R on Nu_0 and Nu_1respectively. It show that, increasing R, makes Nu_0 decrease while Nu_1 enhances with growing R.

7. Conclusion

Free convective heat transfer flow of MHD within two parallel walls in the present of thermal radiation aided by slip velocity convective temperature at the boundary has been deliberated using appropriate fixed parameters. Effects of pertinent parameters on the velocity, temperature, skin friction and Nusselt number profiles are shown discussed through graphs. The findings revealed that:

i. Numerical and analytical solutions agreed for sufficient value of time t.
ii. Velocity and temperature upturn with increasing Gr, R, λ, C_T and B_{i1} but decay with increasing M and Pr.
iii. Skin friction upturns at y = 0 with growing $time\ t, R, M,$ and C_T but drops for increasing $B_{i1}, \lambda,$ and Gr.
iv. Increase in $B_{i1}\ and\ \lambda$ at y = 1 leads to increase in skin friction.
v. Nusselt number decreases with increasing time t and C_T at left plate ($y = 0$) but increases at right plate ($y = 1$).
vi. Increase in B_{i1} and R lead to increase in Nusselt number at left and right plates (y = 0).
vii. Nusselt number enhances at y = 0 with growing Pr but decreases at y = 1.

References

[1] Venkateswarlu M. and Venkata L. D., Slip velocity distribution on MHD oscillatory Heat and mass transfer flow of a viscous Fluid in a parallel plate channel, Ganit *J. Bangladesh Math. Soc.* (2016) (ISSN 1606-3694) Vol: 36 PP: 91-112.

[2] Martin M. J., Boyd I. D., Momentum and heat transfer in laminar boundary layer with slip flow, Journal of Thermo physics and Heat Transfer; (2006) 52: 710–719.

[3] Mehmood A., Ali A., The effect of slip condition on unsteady MHD oscillatory flow of a viscous fluid In a planer channel, Rom. Journ. Phys., (2007) Vol. 52, Nos. 1–2, P. 85–91.

[4] Pal D. and Shivakumara I. S., Mixed convection heat transfer from a vertical heated plate embedded in a sparsely packed porous medium, International Journal for Applied Mechanical Engineering. (2008); 11: 929–939.

[5] Bhattacharyya K, Mukhopadhyay S, Layek G. C., MHD boundary layer slip flow and heat transfer over a flat plate, Chin Phys Lett.; (2011) 28: 024701–024704.

[6] Mohammad A. H, Anwar H. A. and Mohammad A. A., The Effect of Slip Velocity and Temperature Jump on the Hydrodynamic and Thermal Behaviors of MHD Forced Convection Flows in horizontal Micro channels, Iranian Journal of Science and Technology: Transactions of Mechanical Engineering (2016) DOI: 10.1007/s40997-016-0004-x.

[7] Gnaneswara R. M., Velocity and thermal slip effects on MHD third order blood flow in an irregular channel though a porous medium with homogeneous/heterogeneous reactions, Nonlinear Engineering (2017) 6 (3): 167–177 doi.org/10.1515/nleng-2017-0008.

[8] Mohamed A. and Ahmed A. A., Influences of Slip Velocity and Induced Magnetic Field on MHD Stagnation-Point Flow and Heat Transfer of Caisson Fluid over a Stretching Sheet, Mathematical Problems in Engineering, (2018) Volume 2018, Article ID 9402836, 11 pages https://doi.org/10.1155/2018/9402836

[9] Ellahi R., Sultan Z. A., Abdul B. and Majeed A., Effects of MHD and slip on heat transfer boundary layer flow over a moving plate based on specific entropy generation, Journal of Taibah University for Science, (2018) 12: 4, 476-482, DOI: 10.1080/16583655.2018.1483795.

[10] Manjula D and Jayalakshmi K, Slip Effects on Unsteady MHD and Heat Transfer Flow over A Stretching Sheet Embedded with Suction in A Porous Medium Filled With A Jeffrey Fluid". International Journal of Research (2018) ISSN NO: 2236-6124.

[11] Sheikholeslami M, Kataria H. R. and Mittal A. S., Effect of thermal diffusion and heat-generation on MHD Nano fluid flow past an oscillating vertical plate through porous medium, J Mol Liq. (2018); 257: 12–25.

[12] Nandal J. and Kumari S., The effect of slip velocity on unsteady peristalsis MHD blood flow through a constricted artery experiencing body acceleration, *Int. J. of Applied Mechanics and Engineering, (2019), vol. 24, No. 3, pp. 645-659,* DOI: 10.2478/ijame-2019-0040.

[13] Mohammad M. R, Behnam R., NavidF and Saeid A, Free convective heat and mass transfer for MHD fluid flow over a permeable vertical stretching sheet in the presence of the radiation and buoyancy effects, Ain Shams Engineering Journal (2014) 5 (3): 901–912 http://DOI:10.1016/j.asej.2014.02.007

[14] Wubshet I, The effect of induced magnetic field and convective boundary condition on MHD stagnation point flow and heat transfer of upper-convected Maxwell fluid in the presence of nanoparticle past a stretching sheet, Propulsion and Power Research (2016) pp 164-175 https://doi.org/10.1016/j.jppr.2016.05.003

[15] Siti S P M I, Norihan M. A, Roslinda N, Norfifah B, and Fadzilah M. A., The effect of convective boundary condition on MHD mixed convection boundary layer flow over an exponentially stretching vertical sheet, Journal of Physics: Conf. Series (2017) 949 012016 http//doi:10.1088/1742-6596/949/1/012016

[16] Yahaya S D, Zainal A, Zuhaila I and Faisal S., Effects of slip and convective conditions on MHD flow of Nanofluid over a porous nonlinear stretching/shrinking sheet, Australian Journal of Mechanical Engineering (2018) vol. 16 pp 213-229 https://doi.org/10.1080/14484846.2017.1358844

[17] Dulal P. and Babulal T., Influence of hall current and thermal radiation on MHD convective heat and mass transfer in a rotating porous channel with chemical reaction, International Journal of Engineering Mathematics, (2013) Article ID 367064, 13 pp.

[18] Misra J. C and Sinha A., Effect of thermal radiation on MHD flow of blood and heat transfer in a permeable capillary in stretching motion, Heat and mass transfer, (2013) vol. 49, pp. 617-628.

[19] Kalidas D., Radiation and melting effects on MHD boundary layer flow over a moving surface, Ain Shams Engineering Journal, (2014) vol. 5, pp 1207-1214 https://doi.org/10.1016/j.asej.2014.04.008

[20] Kho Y B, Hussanan A, Mohamed M. K A, Sarif N. M, Ismail Z. and Salleh M. Z, Thermal radiation effect on MHD Flow and heat transfer analysis of Williamson Nano fluid past over a stretching sheet with constant wall temperature" Journal of physics conference series vol. 890 pp. 8-10.

[21] Isah B. Y, Jha B. K, Lin J. E., On a Couette Flow of Conducting Fluid, International Journal of Theoretical and Applied Mathematics, (2018) Vol. 4, No. 1, pp. 8-21. doi: 10.11648/j.ijtam.20180401.12.